

**DOUBLE BARS IN DISK GALAXIES:
DYNAMICAL DECOUPLING OF NON-SELF-GRAVITATING GASEOUS BARS**

Clayton Heller and Isaac Shlosman

University of Kentucky, Lexington, KY 40506-0055, U.S.A.
email: cheller@pa.uky.edu and shlosman@pa.uky.edu

and

Peter Englmaier

*Max-Planck-Institut für Extraterrestrische Physik, Karl-Schwarzschild-Strasse 1, Postfach 1312, Garching,
Germany D-85741*
email: ppe@mpe.mpg.de

ABSTRACT

We find that nuclear rings in barred galaxies can be subject to a new type of non-self-gravitational dynamical instability. The instability leads to the formation of *gaseous* molecular bars with pattern speeds which are substantially *slower* than speeds of the primary *stellar* bars. This spectacular decoupling of nuclear bars from the underlying gravitational potential is triggered but is not driven by the gas viscosity. We find that low-viscosity systems can spend a substantial period of time in a fully decoupled state, with the nuclear bar slowly tumbling in the gravitational field of the primary bar. Higher viscosity systems form nuclear bars which librate about the primary bar. The shape of a nuclear bar, i.e., its eccentricity, correlates strongly with the angle between the bars. We also find that such decoupling, partial or full, most probably will be associated with bursts of star formation and with gas inflow across the inner (Lindblad) resonance zone towards smaller radii.

Subject headings: galaxies: evolution – galaxies: ISM – galaxies: kinematics & dynamics – galaxies: starburst – galaxies: structure – hydrodynamics

1. Introduction

Still unknown, but a substantial fraction of disk galaxies exhibit a phenomenon of double bars, stellar and gaseous (e.g., Shaw et al. 1995; Friedli et al. 1996; Erwin & Sparke 1999; Kenney 1997; Jogee 1999; Marquez et al. 1999; Maciejewski & Sparke 2000; Maiolino et al. 2000). The primary bars extend for several kpc and in most cases define the galactic morphology. The secondary (nuclear) bars, typically less than 1 kpc in extent, are observed only at moderately high spatial resolution, either in the near-infrared or through the CO tracer of molecular gas. However, in order to study their kinematics, an HST-level of resolution is crucial. Both bar types are expected to have a profound effect on the gas flow on corresponding spatial scales and, therefore, on the galactic evolution. Gas is known to fuel activity, stellar and nonstellar, but nowhere else in a galaxy can it influence the overall dynamics to such an extent as in the central regions. Gasdynamics in primary bars was investigated in great detail, including its effects on the overall galactic evolution (e.g., Pfenniger 1996). Gas flow in the nuclear bars is largely assumed to be similar and a scaled-down version of the flow in the large stellar bars (e.g., Regan & Mulchaey 1999). The validity of this approximation, however, is not based on theoretical analysis.

Despite the obvious importance of the nested bars configuration, our understanding of its formation, dynamics and evolution is very limited. Moreover, little work has been performed so far to address the specifics of flow in gaseous as compared to stellar bars. Even the sense of rotation of nuclear bars and their pattern speeds have never been detected directly from observations.

Theoretically, three options exist. First, if the nuclear bar was formed via self-gravitational instability (in the stellar or gaseous disks), it must spin in the direction given by the angular momentum in the disk, i.e., in the direction of the primary bar (Shlosman, Frank & Begelman 1989). In this case, the pattern speed of the nuclear bar, Ω_n , will be substantially *higher* than that of the primary bar, Ω_p . This was confirmed in numerical simulations which included the gas self-gravity (Friedli & Martinet 1993; Combes 1994; Heller & Shlosman 1994). The best arrangement corresponds to the corotation radius of the nuclear bar being approximately equal to the radius of the Inner Lindblad resonance (ILR) of the primary

bar, reducing the fraction of chaotic orbits (Pfenniger & Norman 1990). The gas presence appears to be imperative for this to occur (Shlosman 1999 and refs. therein). In this case, both bars are dynamically *decoupled* and the angle between them in a face-on disk is arbitrary.

Second, two bars can co-rotate, being dynamically *coupled* and their rotation completely synchronized. Such a configuration can be a precursor to the future decoupled phase (discussed above), or continue indefinitely (e.g., numerical simulations of Shaw et al. 1993; Knapen et al 1995). The nuclear bar is expected to lead the primary bar in the first quadrant at a constant angle, close to 90° . An explanation for this phenomenon lies in the existence of two main families of periodic orbits in barred galaxies, the so-called x_1 orbits aligned with the primary bar and the x_2 orbits which are perpendicular to it (e.g., Binney & Tremaine 1987). The gas losing angular support due to the gravitational torques from the primary bar will flow towards the center and encounter the region with the x_2 orbits, which it will populate¹. The extent of the x_2 family defines the inner resonance region in the disk, i.e., position of the nonlinear inner and outer ILRs. The nuclear bar may be further strengthened by the gas gravity, which drags stars to x_2 orbits. However, the amount of gas accumulating in the ILR resonance region may be insufficient to cause the dynamical runaway. In this latter case, it is thought that the synchronized system of two nearly perpendicular bars can be sustained indefinitely, until star formation or other processes cease it.

Third, the secondary bar can rotate in the opposite sense to the primary bar. This situation may arise from merging, when the outer galactic disk acquires opposite angular momentum to that of the inner disk. It was considered by Sellwood & Merritt (1994) and Davies & Hunter (1997) and appeared as a non-recurrent configuration. At least one of the bars should be purely stellar, because the gas cannot populate intersecting orbits.

Although all three options discussed above have specific predictions verifiable observationally, the triggering mechanism(s) for the formation of such systems require much better understanding. To close this gap, we analyze the decoupling process of nuclear bars in disk galaxies. Here we show that dy-

¹Strictly speaking, the gas will not occupy the perfectly periodic orbits because of dissipation, but will be found at nearby energies, which is sufficient for our discussion

namical evolution does not stop with the formation of two coupled perpendicular bars (as described above), *even* when gas self-gravity is neglected. Instead, partial or complete decoupling of a nuclear gaseous bar, depending on the degree of viscosity in the gas, is triggered for a prolonged period of time. This bar either librates around the major axis of the primary bar, or acquires a different pattern speed, which is substantially *slower* than that of the primary bar. Our work is complementary to studies which focused on large-scale gas dynamics in barred galaxies, and, due to the limitations of the numerical schemes, did not resolve the central regions discussed here (e.g., Athanassoula 1992). The role of gas self-gravity in the decoupling process is fully worked out in a subsequent paper, and in this case $\Omega_n > \Omega_p$. Both regimes are likely to be relevant to our understanding of galactic evolution.

Section 2 details the formation of the nuclear gaseous bar and its subsequent decoupling from the primary bar. Section 3 discusses the physical reasons for this evolution and possible observational implications for disk galaxies.

2. Nuclear Bar Evolution: Librations About the Primary Bar and Complete Decoupling

In our study, the disk and its bulge/halo are represented by Miyamoto & Nagai (1975) analytic potentials

$$\Phi = -\frac{GM}{\sqrt{r^2 + (A+B)^2}}, \quad (1)$$

where M — mass in units of $10^{11} M_\odot$ and A, B — spatial scaling parameters, in units of 10 kpc, are given in Table 1.

The large-scale stellar bar is given by the Ferrers' (1877) potential with $n = 1$ and rotates with a prescribed pattern speed Ω_p . In dimensionless units, its mass and semi-major (a) and semi-minor (b) axes are 0.18, 0.22 and 0.05, respectively. The dynamical time $\tau_{\text{dyn}} = 1$ corresponds to 4.7×10^7 yrs. The gas is evolved using a 2D version of a Smooth Particle Hydrodynamics (SPH) code (details in Heller &

Table 1: Model Parameters (see text)

Component	Mass	A	B
disk	1.0	0.4	0.1
bulge	0.3	0.0	0.1

Shlosman 1994) neglecting the gas self-gravity, and, alternatively, using the grid code ZEUS-2D (Stone & Norman 1992).

The bar potential is turned on gradually to avoid transients. The pattern speed $\Omega_p = 1.1$ and the bar strength are chosen to form a double ILR in the disk and allow the primary bar to end near the Ultra-Harmonic resonance at $r = 0.7$, with corotation at $r = 0.9$. Formation of the ILRs is verified using non-linear orbit analysis (see Heller & Shlosman 1996). Along the primary bar major axis the outer ILR is found at $r = 0.14$ and inner ILR at 0.05. Note, that due to the primary bar strength, linear analysis gives erroneous results about positions of the ILRs. Gas sound speed is taken to be 10 km s^{-1} .

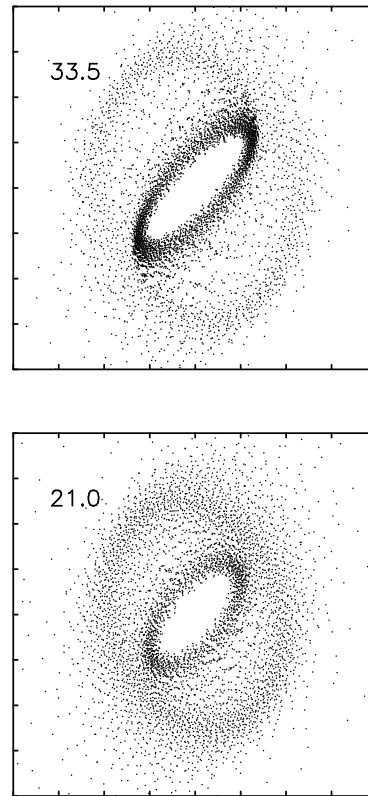


Fig. 1ab.— Representative frame in the evolution of (a) the Standard model (upper) (Seq. 1) and (b) high-viscosity model (lower) (Seq. 2). See Fig. 1c captions and the text for future details. The animation sequences discussed here are available in the online edition of the Journal.

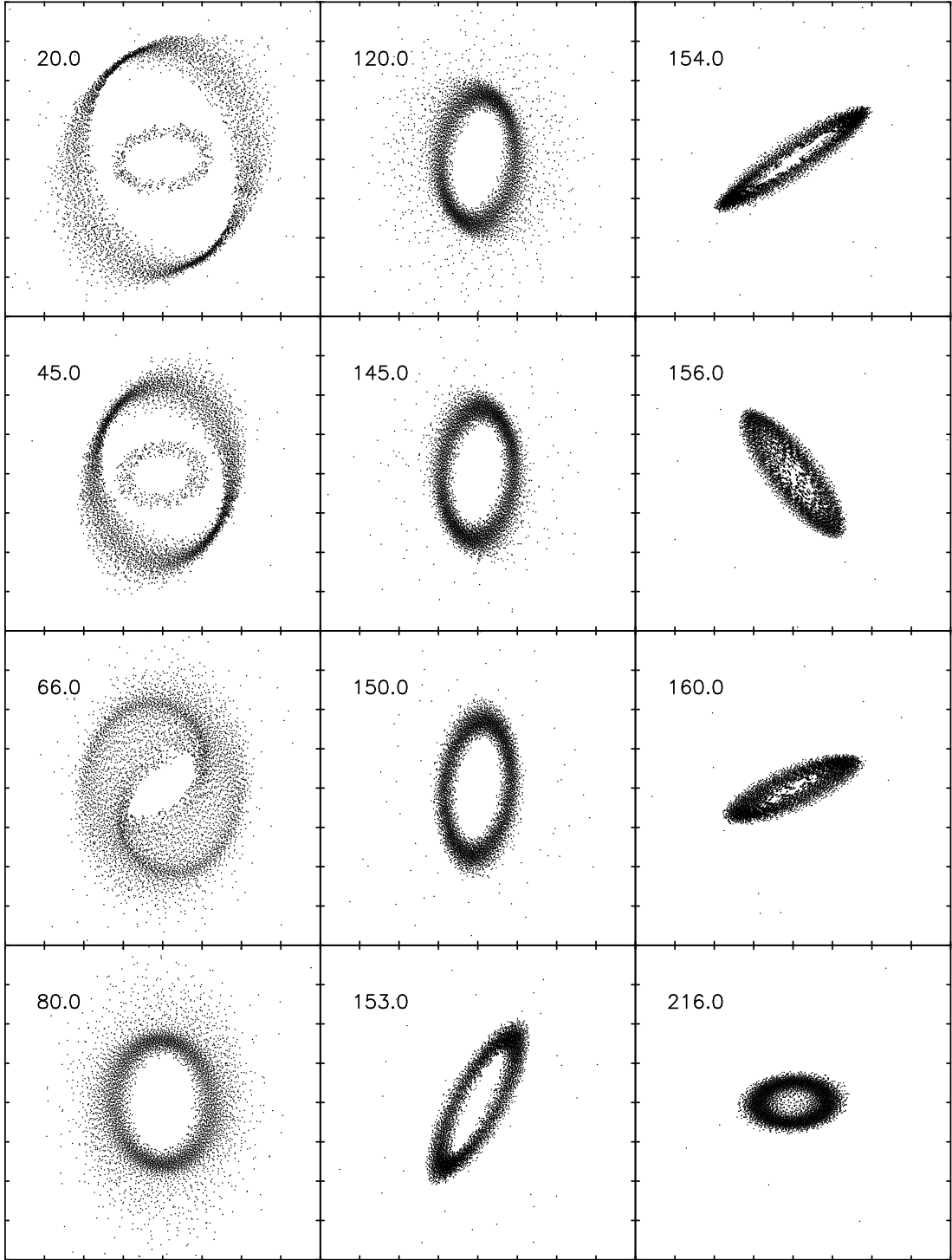


Fig. 1c.— Time evolution of the low-viscosity model (Seq. 3): 2D SPH simulation in the background gravitational potential of a barred disk galaxy (shown face-on). The gas response to the bar torquing is shown in the primary bar frame. The primary bar is horizontal and the gas rotation is counter-clockwise. Note a fast evolution after $t \sim 150$, when the nuclear bar decouples and swings clockwise (!). The bar is ‘captured’ again at $t \sim 211$. Time is given in units of dynamical time τ_{dyn} . The animation sequences discussed here are available in the online edition of the Journal.

The evolution of our Standard model is shown in the animated Sequence 1 in the frame of the primary bar. We ran two additional models with identical initial conditions to that in the Standard model. The *only* difference is that the value of viscosity was changed by a factor of 2, up and down (hereafter ‘high’ [Seq. 2] and ‘low’ [Seq. 3] viscosity models). This was achieved by varying the coefficients of viscosity α and β in the prescription given by Hernquist & Katz (1989). As expected, the gas responds to the gravitational torque from the bar by forming a pair of large-scale shocks, loses its angular momentum and accumulates in a double ring (corresponding roughly to the inner and outer ILRs, see below). In Seqs. 1 (also Fig. 1a) and 2 (also Fig. 1b), both rings interact hydrodynamically and as a result, the outer ring is destroyed and its gas flows into the inner (nuclear) ring. In the low viscosity model (Seq. 3 and Fig. 1c), the inner ring is destroyed and its gas is mixed with the outer ring at intermediate radii. After merging, a single oval-shaped ring corotates with the primary bar, leading it by $\phi_{\text{dec}} \sim 50^\circ$ (hereafter, the angle at decoupling) for the high-viscosity Seqs. 1 and 2, and by $\sim 85^\circ$ for the low-viscosity Seq. 3. The angle ϕ_{dec} while depending on the gas viscosity, is always located in the first quadrant.

Next, the remaining ring becomes increasingly oval and barlike (Figs. 2a,b), its pattern speed changes abruptly, and it swings towards the primary bar, *against* the direction of rotation of this bar. We describe the evolution of this gas flow in terms of the bar dynamics and call it a nuclear bar. (In the inertial frame, the nuclear bar still spins in the same direction as the main bar, albeit with a smaller pattern speed than Ω_p .) The shape of this bar can be described by its axial (minor-to-major) ratio which reaches a minimum when both bars are aligned. After crossing the primary bar axis into the 4th quadrant, the nuclear bar initially decreases its axial ratio, i.e., becomes less oval. Thereafter it stops, becomes more oval and speed up in the prograde direction. The bar axial ratio is reaching its minimum when both bars are aligned and the gaseous bar rotates in the retrograde direction (in the primary bar frame!). Hence, in Seqs. 1 and 2, the nuclear bar librates about the primary bar with a decreasing amplitude, being damped more strongly in the higher-viscosity model. The low-viscosity Seq. 3, however, behaves in a qualitatively different way. Instead of librating about the primary bar, the nuclear bar continues to swing in the same

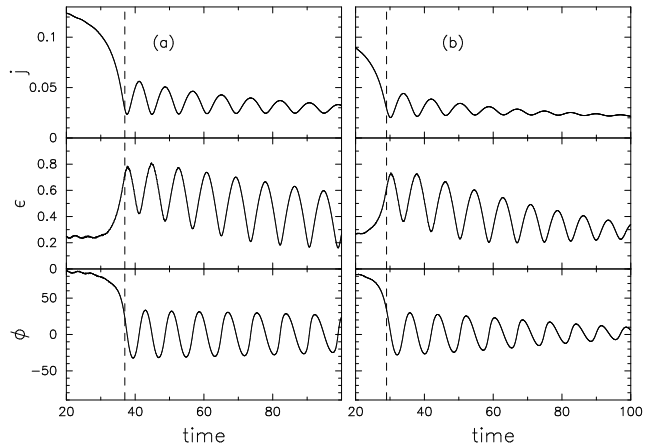


Fig. 2ab.— Standard (a) and high viscosity (b) models: evolution of total specific angular momentum j in the primary bar frame of reference (upper), eccentricity $\epsilon = 1 - b/a$ (middle) and position angle ϕ of the line of apses (lower) of the gaseous nuclear bar. Both ϕ and ϵ were computed from the tensor of inertia of gas within $r \leq 0.2$. The time is give in units of τ_{dyn} . The vertical dashed lines show the end of the merging process between the rings.

direction maintaining a pattern speed $\Omega_n < \Omega_p$ for about 60 dynamical times, corresponding in our units to about $2 - 3 \times 10^9$ yrs (Figs. 1c, 2c). On average, its pattern speed is about half of Ω_p , oscillating around this value with a substantial amplitude. At times, Ω_n is very small, giving the impression that the nuclear bar stagnates in the inertial frame of reference. With time, the eccentricity of the nuclear bar gradually decreases and the bar is trapped again by the valley of the potential of the main bar, thus entering the libration phase, similar to Seqs. 1 and 2.

This behavior of a nuclear gaseous bar, its formation and librations, and especially the kinematically decoupled phase of evolution was never previously observed in numerical simulations. In the following we provide a theoretical explanation for this phenomena within the framework of orbital dynamics in disk galaxies.

3. Discussion: Non-Self-Gravitating Nuclear Gaseous Bars as Slow Rotators

In this paper we neglect the self-gravitating effects in the gas. This situation can be encountered in the early type and/or gas deficient barred disks. A large-

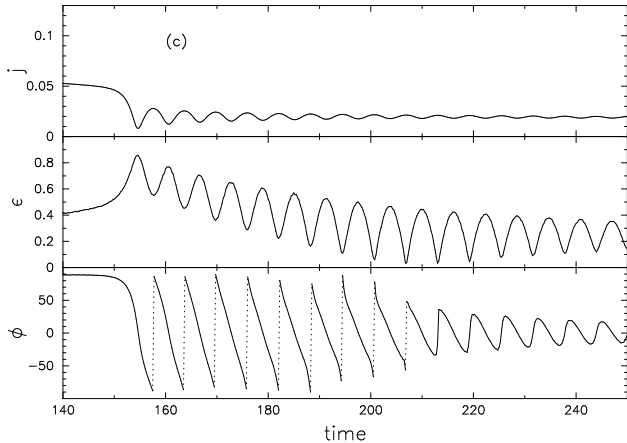


Fig. 2c.— Low-viscosity model: as in Figs. 1a,b. Angle ϕ is shown between $\pm\pi/2$ for presentation only and discontinuities are marked by vertical dotted lines. Full decoupling of the nuclear bar exists at $\tau \approx 150 - 211$.

scale bar in such a galaxy torques the gas, which falls towards the central kpc accumulating in the vicinity of the ILR(s) in the form of a nuclear ring. If the gas surface density and the overall gas accumulation in the ring are small enough, both local and global self-gravitational instabilities will be suppressed. This is the situation we envision. Note, that the positions of ILRs are model-dependent and reflect the overall mass distribution in a galaxy. If the ILRs are absent initially, this will not affect the instability discussed here, as they will form quickly in response to a growing central mass concentration (e.g., Hasan & Norman 1990). The evolution in all models was similar in the SPH and ZEUS-2D codes, hence only the former is shown.

The high resolution and our emphasis on the gas kinematics in the inner resonance region of disk galaxies allow us to study the evolution of nuclear gas with different viscosities. All models, after some intermediate evolution lead to the formation of a single ring, which quickly acquires a barlike shape with well-defined major and minor axes, and librates or precesses rigidly with a pattern speed independent of radius (although the shape is constantly varied). We, therefore, treat this configuration as a bar in all respects. Gaseous bars differ of course from the stellar bars in that the gas can only reside on noninter-

secting and/or not excessively curved orbits. Otherwise, shocks develop and the gas quickly depopulates these orbits. This difference extends also into non-self-gravitating regime.

The most dramatic behavior of gaseous bars in our models is observed in the least viscous system. Here, in the primary bar frame, the nuclear bar decouples and swings in the retrograde direction until being captured again by the primary potential valley. In the inertial system, it spins in the prograde direction, but its Ω_n is much smaller than Ω_p . The precession rate of the gaseous bar is the averaged precession rate of orbits within it, which depends both on the underlying potential *and* the shape of the orbit. Models with a higher viscosity show nuclear bar relaxation towards the primary bar in the form of damped librations.

Why is the gaseous bar precessing as a solid object despite the absence of self-gravity? A simple exercise, of replacing the SPH gas by collisionless ‘stellar’ particles, shows that in such a case each particle orbit precesses at a slightly different rate and the bar dissolves into an axisymmetric configuration in a few orbital times. Hence, a corresponding *stellar* bar without self-gravity cannot exist. But in the limit of weak gravity, it will have a confining effect on stars as well as on gas, and our conclusions will still hold. Addressed elsewhere will be the case of a dominant gravity, when self-gravitational modes are excited with pattern speeds well above Ω_p and overtake the other modes.

It is clear, therefore, that it is the ‘fluid’ (i.e., collisional) nature of the gas which acts to preserve the bar despite the presence of internal shear whose effect is to widen the flow. This process does *not* lead to circularization of the orbits because the background potential does not admit circular orbits. Dependence of bar eccentricity on radius also contributes to the shear, which manifests itself in the gradual azimuthal shift of lines of apses for individual orbits in the bar. At other azimuths, however, the orbits are re-focused again, preventing the bar from dissolving. Because the gas is not self-gravitating in our approximation, the gravity cannot cause the apse alignment and rigid precession of the ring, using the mechanism of Godreich & Tremaine (1979). Instead, this re-focusing is purely hydrodynamical in nature and involves the action of oblique shocks (hydrodynamical torques, i.e., bulk viscosity) in the flow. Of course, such confinement results in the loss of energy by the flow, which is radiated away by the isothermal gas in the sim-

ulations. This loss of energy by the gas leads to non-conservation of Jacobi energy E_J along the orbit.² Before the rings merge, this effect is largest on the outer ring because it forms at energies where the shear is larger. After merging, the remaining ring slowly migrates to lower energies until it encounters the inner ILR, becomes barlike and decouples.

Next we address the physical reasons for the partial or complete runaways shown in each model. The concept of periodic orbits in barred potentials is central to our understanding of both the stellar and gas dynamical evolution in these systems. Most importantly, the families of periodic orbits x_1 and x_2 , mentioned in section 1, are oriented differently with respect to the large-scale bar. Specifically, the x_1 orbits are aligned with the bar between the outer ILR and the corotation radius and between the center and the inner ILR. The x_2 orbits are perpendicular to the bar between the ILRs. The existence of x_2 orbits is a result of the “donkey” effect (Lynden-Bell 1979). A typical orbit will precess with respect to the bar due to the gravitational torques from the latter. These orbits can be ‘captured’ by the bar potential when the precession rate is sufficiently close to Ω_p . Trapped orbits will librate either about the valley of the potential (x_1 orbits), i.e. about the bar major axis, or at right angles to the primary bar (x_2 orbits). As shown by Lynden-Bell, some orbits will speed-up when pulled back by the bar (the “donkey”) and some will slow down in response. The former orbits will have a stable orientation along the minor axis of the bar and contribute to the x_2 family, while the latter will orient themselves along the major axis and contribute to the x_1 family. It is worth reminding that the x_1 and x_2 orbits are resonant orbits and precess with the primary bar pattern speed Ω_p . So in the primary bar frame they do not change their orientation.

The extent of the x_2 orbits can only be determined self-consistently from a nonlinear orbit analysis. Results are presented in Fig. 3 which displays the characteristic curve of the x_2 family for the full range in E_J . For the potential at hand, E_J extends from -4.6 to -2.7 in our units. It is the lower limit in E_J of the x_2 orbits which is important, as evident from the E_J distribution of the SPH particles in the nuclear bar located approximately at the inner ILR at the time of decoupling $\tau = 150$ (Fig. 4). The exact value of

this limit is model-dependent of course, but this is of no importance to the essence of the decoupling.

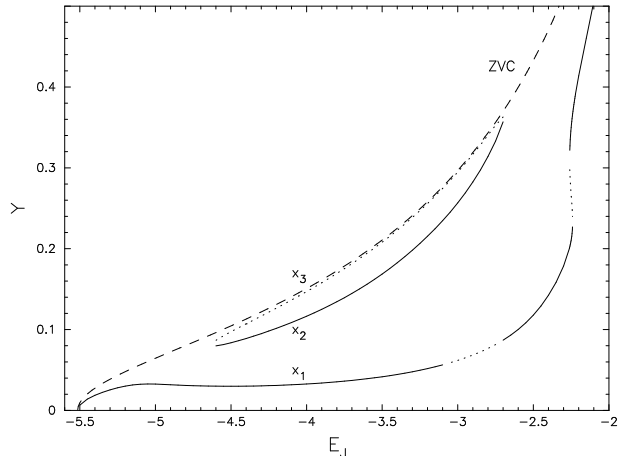


Fig. 3.— Characteristic diagram for the potential and Ω_p used here. The y -axis gives the orbit intercepts along the minor axis of the primary bar. Only x_1 , x_2 and x_3 families are shown. The dotted lines represent unstable orbits. The dashed curve labeled ZVC is the zero velocity curve. The ILRs are located at $E_J = -4.6$ and -2.7 .

As seen in Figs. 1c, 3 and 4, and Seqs. 1-3, the inner ring forms just inside the inner ILR (in E_J and r), on the x_1 orbits and is aligned with the primary bar. Its gas was swept up from orbits within the inner ILR by a positive torque from the primary bar. The outer ring forms between the ILRs, on x_2 orbits of intermediate E_J , and is aligned with the minor axis of the bar. Viscosity is most important during the phase when both rings interact hydrodynamically and merge, which understandably starts earlier and proceeds faster for higher viscosity models. This pre-decoupling evolution is similar in all models, apart from the timescale.

The crucial difference between the models comes from (1) position of the nuclear bar on the E_J axis after the merging, and (2) the value of ϕ_{dec} angle, i.e. the orientation of the nuclear bar at the time of decoupling. For high-viscosity and standard models the gaseous bar is situated very close to the inner ILR at $E_J = -4.6$, with a dispersion of ± 0.1 . The low-viscosity bar resides at -4.5 and is accompanied by an asymmetric ‘high’-energy tail which extends to about $E_J = -3$ (Fig. 4) representing a gaseous ‘envelope’ around the bar (see Fig. 4 and Seq. 3). We

²Jacobi energy is a *conserved* total energy of a gas parcel in the rotating frame of the primary bar when dissipation is neglected (see e.g., Binney & Tremaine 1987 for more details).

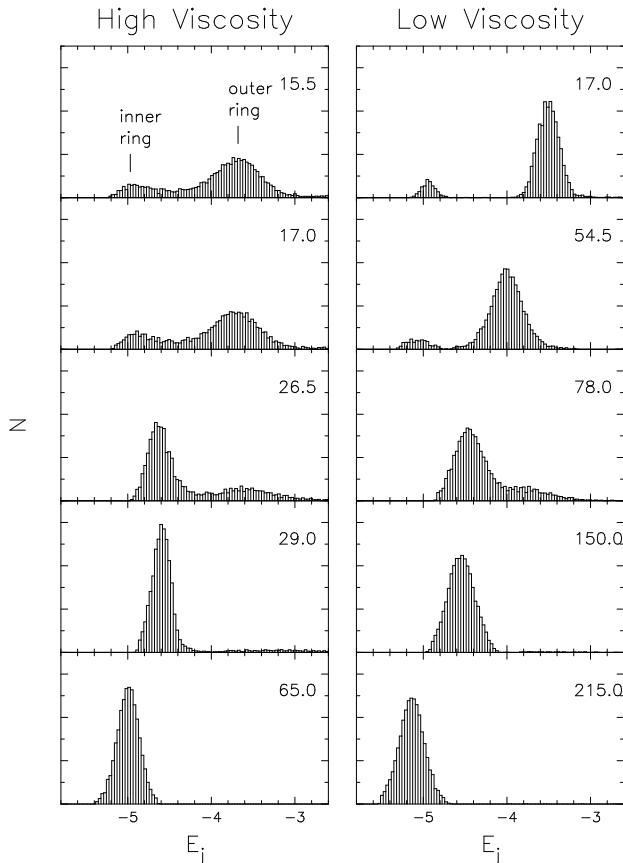


Fig. 4.— Evolution of SPH particle distribution with the Jacobi energy E_J for the high-viscosity (left) and low-viscosity (right) models. The sequence depicts the times of formation of two rings, their pre- and post-merging configurations, decoupling and post-decoupling of nuclear bar. Note that on the left, merging is accomplished at $\tau \approx 29$ after the bar enters libration phase at $\tau \approx 26.5$. The x_2 orbits exist only between $E_J = -4.6$ and -2.7 (Fig. 3).

note that the role of viscosity here is fundamentally different from that in nearly axisymmetric potentials (planetary rings, galactic warps), where it acts to circularize the orbits. In barred potentials, circular orbits do not exist and the gas merely moves from one elongated orbit to another.

The evolution of the inner ring consists of a few phases: formation, merging with the outer ring, migration to the inner ILR, decoupling (partial or full) and post-decoupling. The first phase was discussed above, and the later evolution is addressed below.

The merging with the outer ring mixes high and

low- E_J gas and the ring is ‘lifted’ across the inner ILR, acquiring a leading angle $\phi_{\text{dec}} \sim 50^\circ$ with respect to the primary bar. This is facilitated by a pair of leading shocks in the gas. The single remaining ring is subject to a gravitational torque from the primary bar, which acts to align the ring with the bar. The gas, however, responds to the torque in the following way. The total angular momentum of the gas can be assumed to consist of a circulation along the ring with a high angular velocity Ω and of a much slower precession Ω_n due to the torque from the bar which tumbles with Ω_p . While the latter two frequencies are comparable, they are much lower than Ω . As a result, the circulation along the ring can be treated (roughly!) as an adiabatic invariant. Therefore, the gravitational torque changes the ring’s precession rate and shape but not the internal circulation.

In the pre-decoupling stage, the ring becomes progressively barlike, decreasing its axial ratio. In the low-viscosity model, this gaseous bar resides on purely x_2 orbits and, therefore, responds to the primary bar torque by speeding up its precession while being pulled backwards until it is almost at a right angle to the bar potential valley. Higher viscosity models have gaseous bars forming (after merging) and entering the decoupling phase almost immediately. On the average, the gas in these bars has energies just below that of the inner ILR, where no x_2 orbits exist.

The decoupling happens abruptly when a substantial fraction, $\sim 1/2$, of the gas in the bar finds itself at E_J energies below the inner ILR. The absence of x_2 orbits at these E_J means that the bars either are unable to settle on these orbits (Seqs. 1, 2) or lose their stable orientation along the primary bar minor axis (Fig. 1c and Seq. 3). As a result the nuclear bars enter librations about the main bar with smaller or larger initial departures from the stable orientation along the main bar, *which is a single decisive factor separating the partial and full decouplings*.

The angle ϕ_{dec} is largest for Seq. 3 — the reason for the qualitatively different behavior. All three models show that the gaseous bars in the partial or full decoupling phase experience shape changes depending on their orientation. The bar has a much smaller eccentricity in the 4th quadrant than in the 1st one (Figs. 2a,b,c). Such an asymmetry with respect to the primary bar axis ensures that the resulting gravitational torques from the primary bar are smaller in the 4th quadrant. But only for the least viscous model (Fig. 1c), which has the maximal ϕ_{dec} , does this make

the ultimate difference. In this case the torques are unable to confine the bar oscillation, which continues for a full swing of 2π . The nuclear bar is trapped again at $\tau \sim 211$, after many rotations with respect to the large-scale bar. Fig. 5 shows the dramatic effect the shape change has on the runaway. For comparison, we display the angular momentum of a hypothetical ‘rigid’ bar which is unable to decouple fully.

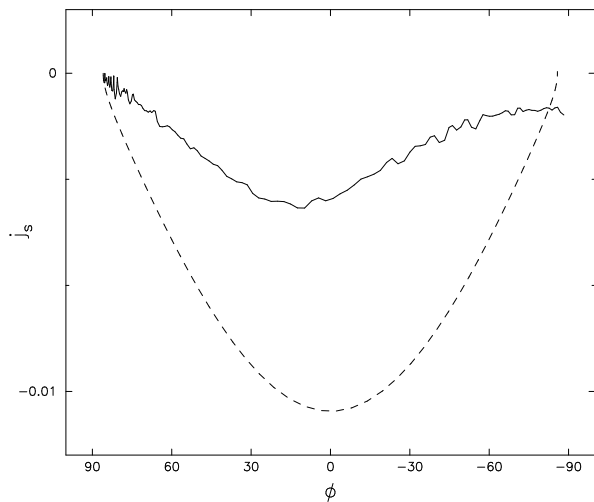


Fig. 5.— Low-viscosity model: specific precession angular momentum j_s of gaseous bar as a function of ϕ during the fully decoupled phase (starting at $\tau = 150$ and $\phi_{\text{dec}} = 85^\circ$; first swing only) in the reference frame of the primary bar. Positive/negative ϕ : the gaseous bar is leading/trailing the primary bar. *Solid line*: actual j_s from the numerical model (the minimum of j_s is shifted from $\phi = 0$ because the moment of inertia decreases with ϕ). *Dashed line*: j_s calculated on the assumption that the shape of the gaseous bar does not change with ϕ (in this case only librations occur).

The clear correlation between the eccentricity of the nuclear bar and its angle with the primary bar in the decoupled phase shown by *all* models can be tested observationally, e.g., by looking on the molecular rings in CO. The maximum in the gaseous bar intensity ϵ is achieved each time both bars are aligned and the minimum occurs when the bars are at right angles.

Two additional effects should have observational consequences as a corollary to decoupling and the periodic increase in ϵ . First, the gas will move inwards across the inner ILR on a dynamical timescale. Shlos-

man et al. (1989) pointed out that the ILR(s) present a problem for radial gas inflow because the gas can stagnate there. A solution was suggested in the form of a global self-gravitational instability in the nuclear ring or disk, which will generate gravitational torques in the gas, driving it towards the nuclear region. This was confirmed by numerical simulations (Knapen et al. 1995; Shlosman 1996).

Recently Sellwood & Moore (1999) resurrected the idea that ILRs will ‘choke’ the gas inflow. However, as we see here, even non-self-gravitating nuclear rings are prone to dynamical instability which drives the gas inwards, whether in a full or partial decoupling. Second, this instability can be accompanied by star formation along the molecular bar due to increased dissipation in the gas, and this star formation will have a quasi-periodic bursting character.

In summary, we have investigated the properties of non-self-gravitating gaseous bars in barred disk galaxies and their formation from nuclear rings and decoupling from the underlying gravitational potential. We found that the degree of viscosity in the gas is a crucial factor in the diverging evolution of these systems, namely, the low-viscosity systems are expected to spend a substantial period of time in a fully decoupled state, with nuclear gaseous bars having much slower pattern speeds compared to the primary bars. The nuclear bar shape is expected to correlate with the angle between the bars. We also find it plausible that gas compression accompanying such decoupling, partial or full, can be associated with bursts of star formation and with gas inflow across the ILRs towards smaller radii. Both gridless and grid numerical codes reproduce the above evolution.

We thank Seppo Laine for his comments. This work was supported in part by NASA grants NAG 5-3841, WKU-522762-98-6 and HST GO-08123.01-97A to I.S., which is gratefully acknowledged.

REFERENCES

- Athanassoula, E. 1992, MNRAS, 259, 345
- Binney, J., & Tremaine, S. 1987, Galactic Dynamics (Princeton Univ. Press)
- Combes, F. 1994, *Mass-Transfer Induced Activity in Galaxies*, ed. I. Shlosman (Cambridge Univ. Press), 170
- Davies, C.L. & Hunter J.H. Jr. 1997, ApJ, 484, 79
- Erwin, P. & Sparke, L. 1999, ApJ, 521, L37

- Ferrers, N.M. 1877, Q.J. Pure Appl. Math., 14, 1
- Friedli, D. & Martinet, L. 1993, A&A, 277, 2
- Friedli, D., Wozniak, H., Rieke, M., Martinet, L. & Bratschi, P. 1996, A&AS, 118, 461
- Goldreich, P. & Tremaine, S. 1979, AJ, 84, 1638
- Hasan H., Norman C.A. 1990, ApJ, 361, 69
- Heller, C.H. & Shlosman, I. 1994, ApJ, 424, 84
- Heller, C.H. & Shlosman, I. 1996, ApJ, 471, 143
- Hernquist, L. & Katz, N. 1989, ApJS, 70, 419
- Jogee, S. 1999, Ph.D. Thesis, Yale University
- Kenney, J.D. 1997, IAU Symp. 184 on *The Central Regions of the Galaxy and Galaxies*, p. 43
- Knapen, J.H., Beckman, J.E., Heller, C.H., Shlosman, de Jong, R.S. 1995, ApJ, 454, 623
- Lynden-Bell, D. 1979, ApJ, 187, 101
- Maciejewski, W. & Sparke, L.S. 2000, MNRAS, 313, 745
- Maiolino, R., Alonso-Herrero, A., Anders, S., Quillen, A., Rieke, M.J., Rieke, G.H. & Tacconi-Garman, L.E. 2000, ApJ, 531, 219
- Marquez, I., Durret, F., Gonzalez Delgado, R.M., Marroero, I., Masegosa, J., Maza, J., Moles, M., Prez, E. & Roth, M. 1999, A&AS, 140, 1
- Miyamoto, M. & Nagai, R. 1975, Publ. Astron. Soc. Japan, 27, 533
- Pfenniger, D. 1996, in Proc. Centennial Nobel Symp. on *Barred Galaxies & Circumnuclear Activity*, Aa. Sandqvist & P.O. Lindblad, Eds. (Springer-Verlag), p. 91
- Pfenniger, D. & Norman, C.A. 1990, ApJ, 363, 391
- Regan, M.W. & Mulchaey, J.S. 1999, AJ, 117, 2676
- Sellwood, J.A. & Merritt, D. 1994, ApJ, 425, 530
- Sellwood, J.A. & Moore, E.M. 1999, ApJ, 510, 125
- Shaw, M.A., Axon, D.J., Probst, R. & Gatley, I. 1995, MNRAS, 274, 369
- Shaw, M.A., Combes, F., Axon, D.J. & Wright, G.S. 1993, A&A, 273, 31
- Shlosman, I. 1996, in Proc. Centennial Nobel Symp. on *Barred Galaxies & Circumnuclear Activity*, Aa. Sandqvist & P.O. Lindblad, Eds. (Springer-Verlag), p. 141
- Shlosman, I. 1999, *Evolution of Galaxies on Cosmological Timescales*, J.E. Beckman & T.J. Mahoney, eds. (ASP Conf. Series), p. 100
- Shlosman, I., Frank, J. & Begelman, M.C. 1989, Nature 338, 45
- Stone, J.M. & Norman, M.L. 1992, ApJS, 80, 753